

Transition to cellular agriculture reduces agriculture land use and greenhouse gas emissions but increases demand for critical materials

Mohammad El Wali ^{1,2,3✉}, Saeed Rahimpour Golroudbary ^{4✉}, Andrzej Kraslawski^{5,6} & Hanna L. Tuomisto ^{1,2,7}

Cellular agriculture, that is, the production of cultured meat and microbial proteins, has been developed to provide food security for a growing world population. The use of green energy technologies is recommended to ensure the sustainability of changing traditional agriculture to a cellular one. Here, we use a global dynamic model and life-cycle assessment to analyze scenarios of replacing traditional livestock products with cellular agriculture from 2020 to 2050. Our findings indicate that a transition to cellular agriculture by 2050 could reduce annual greenhouse gas emissions by 52%, compared to current agriculture emissions, reduce demand for phosphorus by 53%, and use 83% less land than traditional agriculture. A maximum 72% replacement of livestock products with cellular agriculture using renewable energy is possible based on the 2050 regional green energy capacities. A complete transition can be achieved but requires 33% of the global green energy capacities in 2050. Further, the accelerated demand for critical materials will not exceed their primary production capacities, except for tellurium. We conclude that a transition to cellular agriculture is possible with environmental benefits and provide a benchmark to study different alternatives to animal-based diets.

¹ Department of Agricultural Sciences, University of Helsinki, Helsinki, Finland. ² Helsinki Institute of Sustainability Science (HELSUS), University of Helsinki, Helsinki, Finland. ³ Rurality Institute, Faculty of Agriculture and Forestry, Lönnrotinkatu 7, 50100, University of Helsinki, Mikkeli, Finland. ⁴ Hydrometallurgy and Corrosion, Circular Raw Materials Hub, Department of Chemical and Metallurgical Engineering (CMET), School of Chemical Engineering, Aalto University, Espoo, Finland. ⁵ School of Engineering Science, Industrial Engineering and Management (IEM), LUT University, Lappeenranta, Finland. ⁶ Systems Research Institute, Polish Academy of Sciences, Warsaw, Poland. ⁷ Natural Resources Institute Finland (Luke), Helsinki, Finland. ✉email: mohammad.el-wali@helsinki.fi; saeed.rahimpour@aalto.fi

The world is heading towards unprecedented levels of global warming, partially driven by intensive livestock production causing 20% of global anthropogenic greenhouse gas (GHG) emissions¹. We also need to produce around 40% more livestock proteins to meet the global demand in 2050². Therefore, food and agriculture industries have been seeking novel alternatives, such as cellular agriculture, as an emerging branch of biotechnology to mitigate the environmental and animal welfare challenges related to conventional animal farming for meat and dairy production³. Previous studies have shown that protein-rich foods produced by cellular agriculture (e.g., cultured meat and microbial proteins) can be a solution for the problems related to industrial livestock farming by overcoming some of its undesirable consequences, such as global warming, land, and water use^{4–6}. However, cellular agriculture is energy-intensive and might increase industrial energy consumption as it replaces biological systems with chemical and mechanical ones⁷. Hence, using low-carbon energy technologies for cellular agriculture is necessary to maintain the initial objective of decarbonized food systems. This is in line with the global roadmap initiative where ‘green energy’ technologies, e.g., wind and solar-based power, are estimated to make up around two-thirds of worldwide energy production by 2050⁸. It is estimated that the share of electricity in global energy consumption will increase from 19% in 2016 to 49% in 2050, and the share of renewable energy sources will increase from 24% to 86% during the same time period⁸.

Agricultural production, cell-culturing technologies, and green energy generation use raw materials that serve nutritional, structural, and technology-specific purposes^{9–11}. Some of those materials possess very high economic importance, are under high supply risk, and are vulnerable to supply restrictions. Thus, they are classified as critical materials, based on the United States Geological Survey (USGS) and the European Union (EU) commission listings^{12,13}. The rapid growth of technological innovations accelerated the demand for critical materials. This positive correlation between the two phenomena (technological innovations and material usage) has uncovered challenges of sustainability for critical material supply chains¹⁴. Hence, the causal relationship between cellular agriculture practices, green energy technologies, and consumption of critical materials needs to be investigated. This study is driven by a question: to what extent can cell-cultured foods produced with green energy meet global demand for meat and dairy proteins without exceeding the maximum extraction rates of critical material reserves? In addition, what is the impact of this transition on global GHG emissions, agricultural land, and phosphorus consumption?

Here, we assess the availability of critical materials for technologies used in green energy sectors^{10,15}, particularly for cellular agriculture¹⁶. Nutrient inputs are essential during cell-culturing for protein production to provide final products with nutritional benefits comparable to livestock commodities¹⁷. Phosphorus (P) is an essential nutrient for food and human consumption¹⁸. In the green energy sector, critical materials are needed for constructing steel, i.e., chromium (Cr), nickel (Ni), and equipment, such as aluminum (Al), zinc (Zn), and manganese (Mn)¹⁰. For wind power technologies, turbines are heavily reliant on permanent magnets made of critical materials, including mainly boron (B), and rare earth elements (REE), i.e., terbium (Tb), dysprosium (Dy), neodymium (Nd), and praseodymium (Pr)¹⁹. For solar photovoltaic (PV) panels, silicon (Si), germanium (Ge), gallium (Ga), tellurium (Te), and indium (In) are among the critical materials used for building solar cells, depending on the type and technology²⁰. Cellular agriculture production is heavily dependent on stainless steel-based facilities for processing tanks²¹. The stainless-steel structure of the equipment helps to prolong the lifetime of equipment and prevent corrosion. Stainless steel is a

common alloy used in dairy production and wastewater treatment facilities as well. Common steel grades used for these applications include 316 and 304 steel, which contain two critical materials, i.e., Cr and Ni^{22,23}.

This work provided a global assessment of the impact of cellular agriculture on the consumption and the resource capacity of materials such as P, Al, B, Cr, Zn, Ni, Si, Te, Ge, In, Ga, Mn, Tb, Dy, Nd, and Pr. In this study, the primary production capacity refers to the maximum probable output of the extracted material given current facilities and extraction technologies²⁴. The concept of maximum production capacity represents the upper limit of primary production of raw materials that global industry can achieve without incurring additional costs or making changes to its existing infrastructure. We simulated the food system transition from traditional to cellular agriculture and assessed the application of the most common green energy technologies (i.e., wind turbines and photovoltaic panels) in this transition.

The model design followed the system dynamics approach to understand the complexity of systems integration, i.e., food production, energy supply, agriculture land use, GHG emissions, and demand for critical materials. The model is explicitly described in the methods section as well as Supplementary Method 1, Supplementary Tables 3 and 4.

Cellular agriculture refers to culturing animal, plant, or microbial cells in bioreactors to produce alternatives to agricultural products²⁵. Microbial protein (MP) and cell-cultured recombinant proteins (RP) are cellular agriculture products that can be used as substitutes for animal-based proteins in human diets^{26–28}.

We analyzed the application of MP and cell-cultured RP as alternative protein sources. The detailed production processes were considered based on the study by Järviö et al.²⁹ for MP from hydrogen-oxidizing bacteria (Supplementary Data 12) and Järviö et al.³⁰ for cell-cultured RP using “*Trichoderma reesei*” (Supplementary Data 7 and 8).

The transition intended to replace livestock products. MP replaced meat varieties, including cattle, pork, lamb, and poultry, as they deliver high-quality protein comparable to livestock meat proteins³¹. Whereas cell-cultured RPs replaced eggs, dairy (i.e., milk and cheese), and meat varieties as they can deliver the nutritional benefits of egg ovalbumin³⁰, dairy proteins³², and meat proteins²⁸. The transition model to cellular agriculture considered the replacement of livestock products with microbial and cell-cultured recombinant proteins based on the protein contents of commodities. The calculations of the replacement and the protein contents of livestock commodities (i.e., beef, pork, lamb, poultry, milk, cheese, and eggs) can be found in Supplementary Tables 3 and 4.

The scenario analysis was conducted to assess the global transition to cellular agriculture within 30 years (2020–2050), which aligns with the global road-map initiative for a zero-carbon environment⁸. The transition to the studied cellular agriculture products was based on the S-curve gradual adoption process where key players include early adopters, early majority, late majority, and laggards. This process reflects how the consumers perceive novel products entering the market (i.e., early adopters are risk takers, late adopters are risk-averse)³³. The adoption process of the model fades in from 2020 until reaching the saturation stage by 2050. Data on the designed adoption can be found in the annotated code, Supplementary Methods 6 and 7. Keeping in mind that the future production of livestock proteins is influenced by population, income, and livestock demand², we analyzed several scenarios. Starting from a reference scenario where there is no-replacement taking place (Scn0), we developed ten replacement scenarios reaching a 100% replacement of livestock with cellular agriculture (Scn10)—a 10% incremental increase

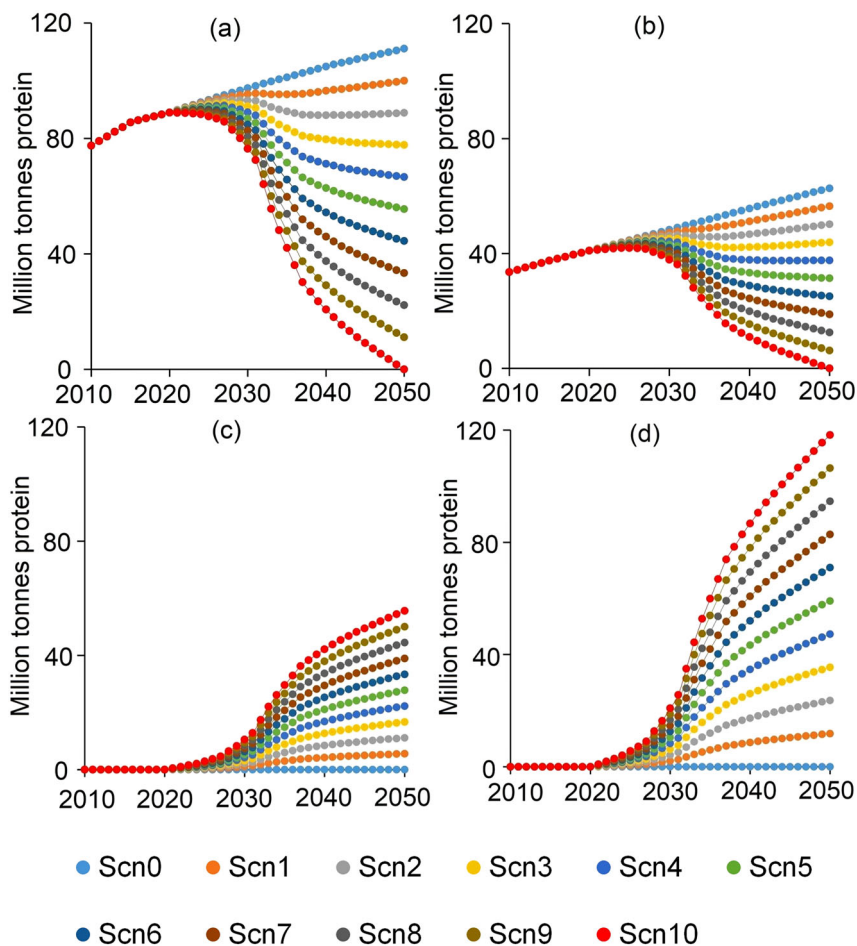


Fig. 1 Global meat, dairy, and egg production (in million tonnes protein) under different replacement scenarios (Scn0→Scn10) between 2010 and 2050. **a** Livestock meat production. **b** Livestock dairy and egg production. **c** MP production. **d** Cell-cultured RP production.

between each two scenarios (Fig. 1a–d). We referred to Humpenöder et al.² in designing the replacement percentages of livestock with cellular agriculture. Humpenöder et al.² assumed a maximum of 80% replacement of ruminant meat with sugar-based microbial proteins. In this study, we aimed for the full replacement of livestock in order to provide the maximum spectrum of changes that can occur in the future.

This research showed the environmental benefits associated with the global replacement of livestock with the studied cellular agriculture products, i.e., MP and cell-cultured RP, powered by green energy technologies. The benefits were characterized by reducing the overall GHG emissions and the agricultural land use associated with the food chain. Moreover, the results indicated a sufficient global capacity of green energy technologies in powering this cellular transition, at least until 2050. Despite the consequences of the cellular agriculture transition on increasing the demand for the associated critical materials, we demonstrated the possibility of such a transition to happen within the global budgets of the studied critical materials. Tellurium was the only exception, where the primary production capacity limits did not allow for >60% global livestock replacement.

Results

Trends in energy consumption in the food system. The energy system assessment covered the demand for critical materials following the changes in green energy supply and facility production, as the system analysis followed the cradle-to-gate

approach for all food and cellular agriculture products, including the raw materials needed for the energy supply and facility production (Supplementary Fig. 1).

The energy required for cellular agriculture includes ‘direct’ and ‘indirect’ energy inputs. The production processes and the related environmental data of cellular agriculture products (i.e., microbial proteins and cell-cultured recombinant proteins), including GHG emissions and direct/indirect energy consumption, were derived from life-cycle assessment (LCA) studies by Järviö et al.^{29,30}. Direct energy refers to the electricity needed for water electrolysis, propagation, fermentation, pasteurization, separation, and drying of the microbial protein product²⁹. For cell-cultured RP, direct energy refers to the electricity needed for cultivation, filtration, purification, and drying of the cultured recombinant protein product, in addition to the electricity required for cleaning³⁰.

Indirect energy includes all the energy needed to produce the raw materials and resources for product manufacturing³⁴. For cell-cultured RP, the indirect energy is used to produce ammonia water, ammonium sulfate, salt mix, antifoaming agent, glucose, and the resources for the electricity used for unit production. For MP, the indirect energy is used to produce nutrients, ammonia water, and the resources for the electricity used for unit production.

Our results showed that the transition to cellular agriculture by 2050 increased the energy demand of global food systems by 69%, reaching around 14.6 petawatt-hours when wind energy was used, and 83% reaching around 15.8 petawatt-hours when solar PV

energy was used for the Scn10 replacement scenario. Around 52–56% of the energy demand originated from MP and cell-cultured RP production (Supplementary Discussion 1, Supplementary Fig. 3). The utilization of either wind or solar PV sources to power the global transition to cellular agriculture leads to different energy demands of the global food system. This was driven by the different indirect energy inputs needed to generate each energy source (i.e., wind and solar PV), where solar PV requires 1.3 times more energy than wind per kWh generated.

Deployment of green energy technologies. In this work, the maximum power output of energy sources is called “energy capacity”. The allocation of green energy capacities to fuel the global transition to cellular agriculture is limited by several factors, such as physical obstacles (e.g., Betz limit for wind turbines or huge surfaces required for solar panels), technical barriers (e.g., shortage of critical materials), and social constraints (e.g., affordability of products or changing consumption patterns). We referred to current global capacities derived from the latest report of British Petroleum (BP)³⁵, in addition to the latest work by Carrara et al.¹⁰, where three future demand scenarios were developed for green energy capacities by the end of 2050, namely: Low- (LDS), Middle- (MDS), and High-demand (HDS) scenarios. The development of these scenarios is based on four major factors: (1) Power generation capacities, (2) Plant lifetime, (3) Sub-technology market shares, and (4) Material intensity. Wind and solar-based energy technologies are considered in the analysis: onshore and offshore turbines for wind-based energy as well as crystalline silicon (c-Si), cadmium telluride (CdTe), copper indium gallium diselenide (CIGS), and amorphous silicon (a-Si) technologies for PV.

Figure 2 represents national and global energy capacity-based analysis of cellular agriculture transition in 2050 (Details on country-level livestock production and local green energy capacities can be found in Supplementary Data 1 and 3). The objective is to determine the regions with the highest potential to lead the way for the transition to cellular agriculture based on the world shares of green energy capacities. Considering the national capacity of energy in 2050, if each country wants to satisfy its demand for cellular proteins, there is a production limit of the required green energy (Fig. 2a). Assessment of the required energy for national cellular agriculture activities shows that a maximum 72% of livestock products can be replaced by cellular proteins in 2050, using wind turbines (37%) and solar PV panels (35%). Around 63% of this transition takes place in Europe, North America, and Northeast Asia (Fig. 2a). The results reflect the unequal distribution of green energy resources, where Europe, Northeast Asia, and North America possess around 70% of wind capacities, while South Asia, East Asia, and North America possess 76% of solar PV capacities worldwide.

Considering global energy capacity, as shown in Fig. 2b, a complete cellular agriculture transition (Scn10) can be achieved by 2050, which requires at most 33% of the global green energy capacities in 2050 (equivalent to 2120 GW and 2500 GW for wind turbines and PVs, respectively for the lowest energy projection scenario¹⁰). The potential increase in the transition percentage by a margin of 27% indicates the capacity of most regions to replace >100% of local livestock production, where extra cellular products are intended for countries with less than 100% replacement percentage (Fig. 2c).

The growth in green energy capacities can facilitate higher transition rates to cellular agriculture. Wind and solar energy capacity levels are estimated to reach 2100–2500 GW under LDS, 3400–4500 GW under MDS, and 7900–12500 GW under HDS by the year 2050¹⁰ (Supplementary Data 2). Considering all the

studied projected world green energy demand scenarios, the development of green energy capacities allows for a full transition to cellular agriculture production by 2050, where wind or solar PV can be solely utilized for the energy supply system (Supplementary Discussion 2, Supplementary Fig. 4), requiring at most 1530 GW and 1265 GW of wind and solar PV capacities, respectively. The provision of additional energy for cellular agriculture from either fully solar PV or fully wind technologies allows us to assess the maximal impact on GHG emissions, agriculture land use, and demand for critical materials. By 2050, 72% (in LDS), 44% (in MDS), and 20% (in HDS) of global wind capacity will be required (Supplementary Fig. 4a–c). For the solar PV panels, 51% (in LDS), 28% (in MDS), and 10% (in HDS) of global solar capacity will be required (Supplementary Fig. 4d–f).

GHG emissions and land used in agriculture production. The assessment of GHG emissions and agricultural land use for all food commodities followed the cradle-to-gate approach with data derived from Poore and Nemecek³⁶, World Food LCA³⁷, Agri-footprint³⁸, and Järviö et al.^{29,30}. The work by Poore and Nemecek³⁶ used the global mean data of the environmental impacts. This included 570 studies across 119 countries.

The results demonstrate that the cellular agriculture transition powered by either wind or solar energy sources reduces annual GHG emissions despite the increase in the overall energy demand. A full transition (Scn10) reduces the annual GHG emissions from the food system by 52%, reaching ~7.4 gigatonnes CO₂-eq in 2050 (Fig. 3a) compared with current annual emissions. This accounts for around 48% of current agricultural emissions. The progression in transition rates decelerates the growth of the cumulative GHG emissions, saving up to 132 gigatonnes CO₂-eq by 2050 under the Scn10 scenario, equivalent to 19% of cumulative emissions by the same year under the Scn0 scenario. Details on the GHG calculations can be found in Supplementary Data 15.

The transition to cellular agriculture would reduce the agricultural land requirements by 83% by 2050, releasing around 9.6 million km² of agricultural land for other uses (Fig. 3b). Land saving is mainly due to the elimination of pasture and grass used for livestock grazing that accounts for 84% of total agriculture land used for livestock production, in addition to crops production needed for livestock farming (Supplementary Fig. 6a, b). Pastures occupy more than 74% of total agricultural land in Scn0, while the rest is arable land. In Scn10, arable lands become the main contributor with 100% of total agricultural land in 2050 (Supplementary Fig. 6c, d). Cellular agriculture requires crop input—particularly cell-cultured RP—as a glucose source³⁰. For the cell-cultured RP, the carbon source was assumed to be glucose produced from maize. The microbial protein production does not require agricultural land as the hydrogen-oxidizing bacteria use CO₂ as a source of carbon. The overall results showed lower demands for maize when cellular agriculture replaced livestock production despite the need for maize inputs to the cell-cultured RP production, reaching 883 million tonnes by 2050 in Scn10, down from 1.2 billion tonnes in 2020. The decline in the overall maize demand was driven by the elimination of livestock production that generally requires 65% of world maize production as animal feed³⁹. The land requirements for glucose production contributed up to 6% of the total arable land area by 2050 in Scn10. Details on the land use calculations can be found in Supplementary Data 20.

Trends in phosphorus flows. The transition to cellular agriculture reduces overall phosphorus consumption in the food value chain. Despite the comparable nutrient fractions in

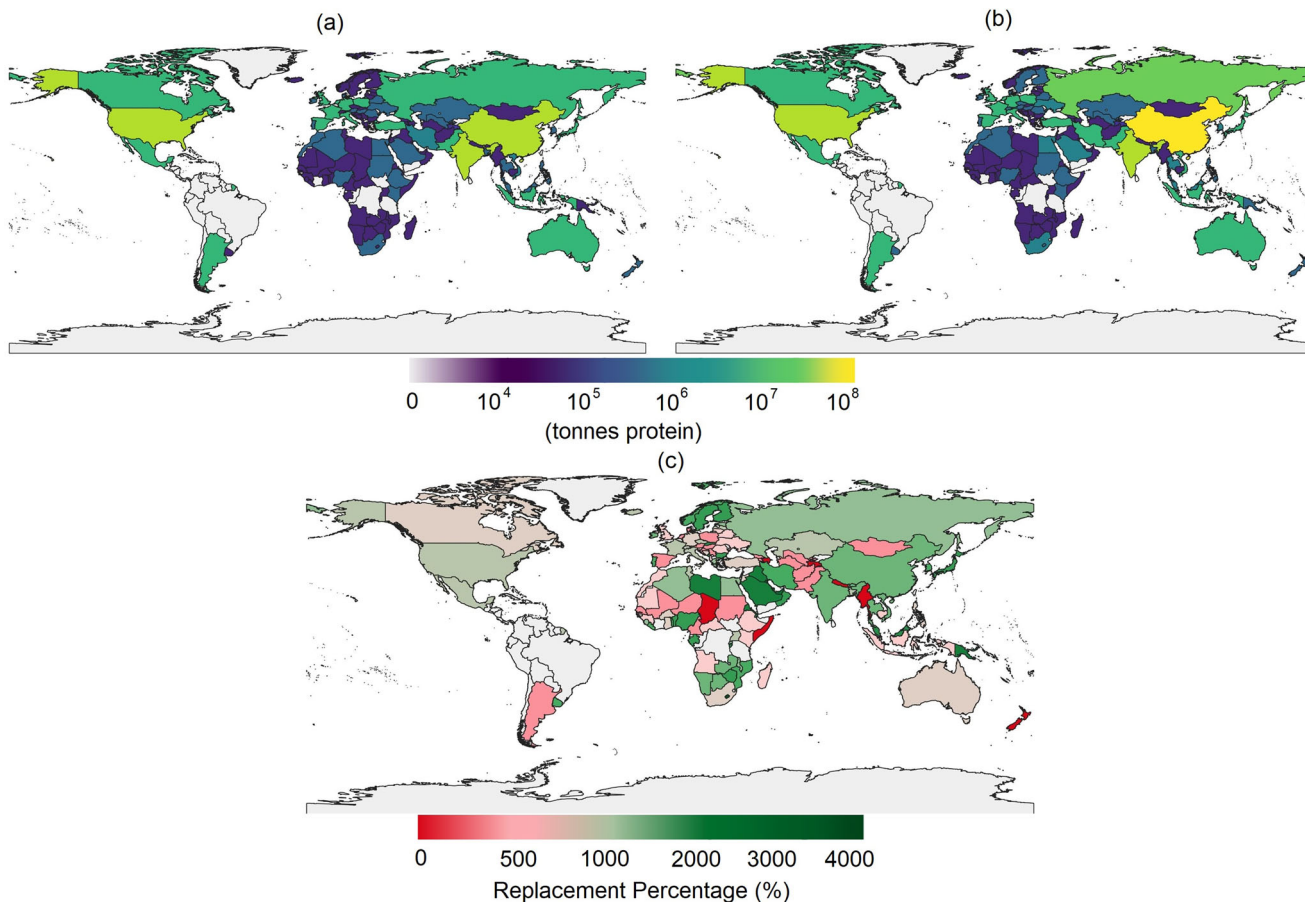


Fig. 2 Projection of the global production of cellular agriculture to replace livestock proteins in 2050 under the 2050 green energy capacity levels. Light grey areas correspond to countries with no available data. **a** Each country aims to replace its own livestock protein production with cellular agriculture proteins as much as possible using local green energy. **b** Each country aims to maximize the production of cellular agriculture proteins based on the availability of local green energy, where extra produced cellular agriculture proteins go for exports. **c** Maximum replacement percentage of local livestock production based on the availability of local green energy. Replacement of livestock proteins includes meat (cattle, poultry, pork, and lamb), dairy (milk and cheese), and eggs.

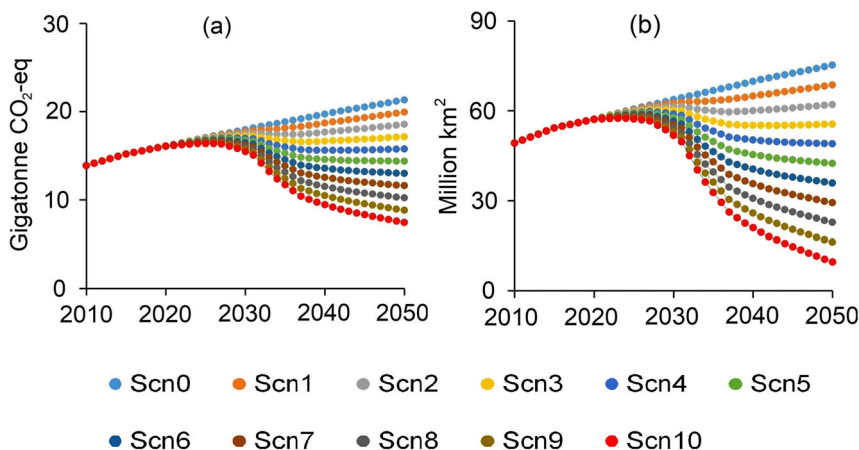


Fig. 3 Environmental impact of the global transition to cellular agriculture under different replacement scenarios (Scn0→Scn10) between 2010 and 2050. **a** Annual greenhouse gas (GHG) emissions from food system. **b** Total agricultural land use from food system.

livestock and cellular agriculture products, the livestock chain experiences several spots of P losses, unlike cellular agriculture production, which is conducted in a precise and controlled environment. The transition to cellular agriculture reduces the primary production of phosphate rock by up to 53% (Fig. 4a). Crop production and nutrient loss are the main flows affected by

the changes in livestock production. The feed used for livestock production accounts for around 41% of the total cereals produced annually⁴⁰. Hence, total crop production is directly affected by declining demand from the livestock sector. Considering a total replacement scenario, total crop production will decrease by 40% in 2050 (Fig. 4b). Along with the food supply chain, the major

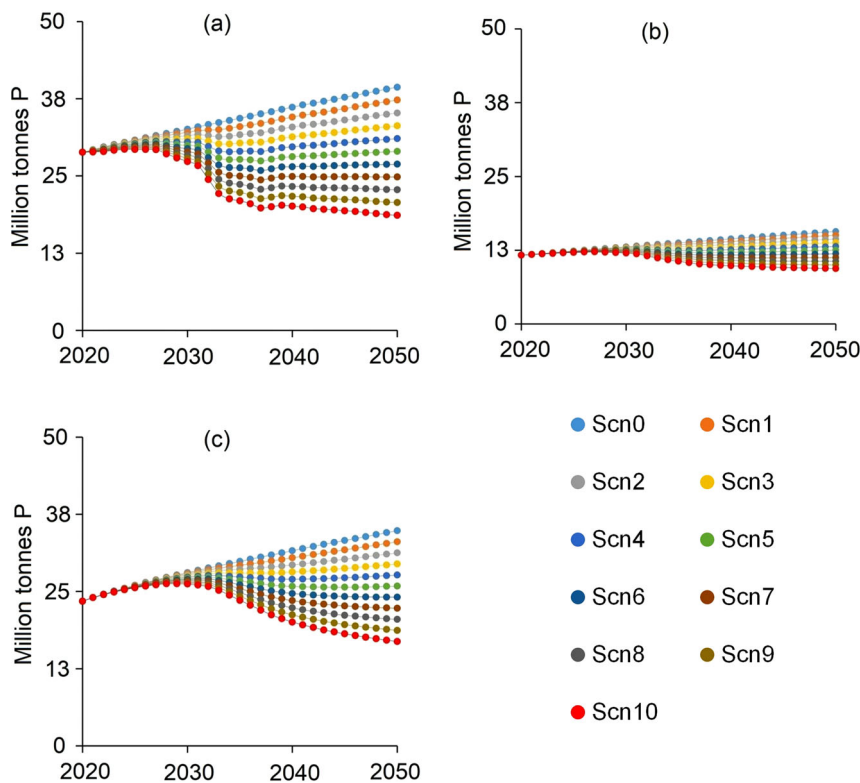


Fig. 4 Global phosphorus flows in a million tonnes P under different replacement scenarios (Scn0→Scn10) between 2020 and 2050. **a** primary production, **b** crop production, and **c** P losses.

losses of nutrients primarily originating from agricultural runoff and livestock waste account for around 47% of the total phosphorus loss. The replacement of livestock with cellular products eases the pressure on cereal production, reducing the magnitude of P losses through waste flows by 51% in 2050 (Fig. 4c).

Demand for green technologies and stainless steel. Following the transition to cellular agriculture, the global demand rises for wind turbines and solar PV panels for green energy generation in the analyzed system, while the growth of stainless-steel demand follows a decline phase by 2050 (Fig. 5).

In 2050, around 68.5 GW of wind energy is projected to be allocated to food production in the case of a 100% replacement scenario compared to 2.6 GW for a no-replacement one (Fig. 5c), reaching 1530 GW of cumulative wind capacity (Fig. 5a). Most of the used wind turbines are onshore, as they continue to dominate the wind power industry (over 88% of global wind energy capacity)¹⁰. Among the list of critical materials used for wind turbine installation in the analyzed system, zinc is the most common material (65% of total critical materials in turbines). This is due to the fact that zinc is used as a component of the coating materials, preventing turbine corrosion⁴¹. Aluminum, manganese, chromium, and nickel contributed to around 33% of the total critical materials applied in wind turbines, as they are used for structural purposes to strengthen turbine construction. Despite the projected decline of the needed structural critical materials due to the future optimization of wind turbines⁴², these materials still constitute the largest share of critical material to be used in wind turbines by 2050. The rest—predominantly REEs and boron—are used in a much smaller amount but are crucial to the operation of wind turbines using permanent magnets¹⁷.

Focusing on solar power, the transition to cellular agriculture increases the demand for PV technologies, reaching up to an

annual production of 50.47 GW in 2050, up from ~1 GW for a no-replacement one. This will lead to an overall installed capacity of 1265 GW (Fig. 5b). It is sufficient to ensure 100% replacement (Fig. 5d). The large gap between the demand levels of turbines and PV panels by cellular agriculture is driven by the amount of electricity to be provided by the specific technologies. Similar to the material intensity levels in wind turbines, structural materials, i.e., aluminum, nickel, and chromium, possess the largest shares of critical material input to the solar PV systems, which is equivalent to 90% of its mineral demand. Silicon is used due to its electrical conductivity. It has the largest demand among the other critical materials, i.e., gallium, tellurium, germanium, and indium, for constructing solar PV systems. The technology of c-Si PV will continue to dominate the solar PV market (up to 95% of total shares) by 2050, despite the introduced alternative PV technologies such as CdTe, CIGS, and a-Si¹⁰.

The variations in installed capacities of wind and solar PV to power the global transition to cellular agriculture stem from multiple factors, i.e., discrepancies in the annual amount of electricity generated per wind turbine and solar PV panel; and the differences in the lifetime of those technologies. Details on the calculation of the annual capacity generation can be found in Supplementary Table 3.

Despite the demand for steel for MP and cultured RP production (e.g., bioreactors and machines for the downstream processes)^{29,30}, the minerals demand for stainless steel needed for food production (dairy and cellular agriculture) and wastewater treatment decreases in the food system if replacement scenarios take place (Fig. 5e). The use of stainless steel for wastewater facilities is the dominant driver of material consumption, accounting for 47% and 52% of total stainless-steel requirements in 2050 with 100% and 0% replacement scenarios, respectively. Stainless-steel consumption decreased by 16% followed by the replacement of dairy products, including milk and cheese, with

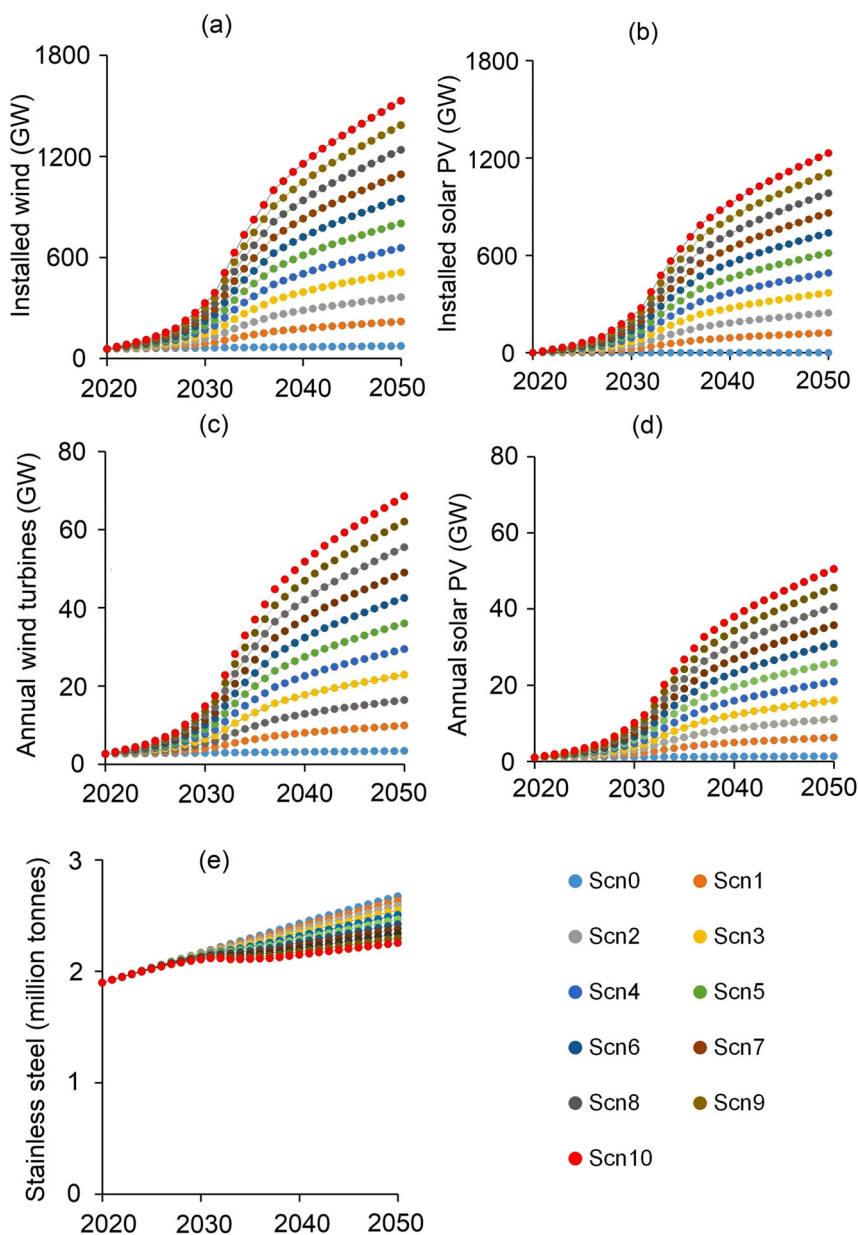


Fig. 5 Global resource requirements for the food system under different replacement scenarios (Scn0→Scn10) between 2020 and 2050. **a** Installed capacity of wind turbines. **b** Installed capacity of solar PV panels. **c** Global annual production of wind turbines. **d** Global annual production of solar PV panels. **e** Global production of stainless-steel for cellular agriculture, dairy, and wastewater treatment facilities in the food system. The average capacity of a wind turbine is 2.75 MW (Supplementary Table 4). The average capacity of a solar PV panel is 315 watts (Supplementary Table 4).

cellular agriculture in Scn10. The annual total demand maintains the increasing trend, following the increase in steel wastewater reservoirs and piping systems to treat waste from human consumption, which is independent of the transition initiatives to cellular agriculture. Details on the wastewater treatment facilities can be found in Supplementary Table 4. Chromium and nickel are the major critical materials utilized in stainless-steel used in dairy, wastewater treatment, and the biotechnological industry. The material intensity of those elements is driven by the grades of the steel used—304 and 316 stainless steel. The consumption of these materials per unit of steel input is not anticipated to experience any changes by the year 2050.

Critical material consumption as part of global flows. The demand for critical materials related to the transition to cellular

agriculture is constrained by the global projections of nutrient flows, stainless steel production, and development of wind and solar PV technologies. Global flows of the critical materials in the studied sectors can be found in Supplementary Data 4–6. The results demonstrate the possibility of achieving a total replacement of livestock products with cellular agriculture, powered solely by either wind or solar energy, without experiencing supply shortages by the year 2050 (Supplementary Fig. 7). The annual generation of global wind and solar-based energy will continue to grow to the year 2050, i.e., LDS by 70–100%, MDS by 200%, and HDS by 600%¹⁰. Similarly, the stainless-steel industry is anticipated to grow by 42% by 2050⁴³.

The demand for chromium and nickel in the analyzed system follows the same trend compared to the global trends in the stainless-steel industry. The flows of chromium and nickel in this

system are related to stainless-steel products, where approximately 55% goes to the construction of solar PV and 44% to other sectors, including dairy production, wastewater treatment, and cellular agriculture production (Supplementary Fig. 7).

In a full replacement scenario, the amount of phosphorus needed for protein products will decrease by 10% in 2050, down from 60% of total availability in 2020 (Supplementary Fig. 7). The total availability corresponds to the available amount of phosphorus from all sources, i.e., primary production and recycling. The declining trend reflects the reduction of P losses that take place in the upstream level of the livestock value chain. This also indicates a more efficient chain of protein production via cellular products than current livestock practices, in which phosphorus demand for livestock production accounts for around 63% in 2050, given a no-replacement scenario. It should be noted that the phosphorus flows in the food system are independent of the different scenarios of green energy projections. Hence, no changes are observed with regard to phosphorus consumption under LDS, MDS, and HDS.

Given a total replacement powered solely by wind power technology, the critical elements (REEs, B, Zn, and Mn) used for the wind installations in the food system are estimated to cover up to 51% of total material flows to wind technology under LDS, 35% under MDS, and 15% under HDS by 2050 (Supplementary Fig. 7). These increases from 2% in 2020 follow the S-curve-based gradual adoption of cellular agriculture in the global food system. Similarly, the contribution of critical materials (Ga, Ge, In, Si, and Te) for the solar PV energy in the food system to the global flows increases as the total replacement takes place, accounting for 23% under LDS, 13% under MDS, and 6% under HDS by 2050. In the food system, aluminum is used predominantly in solar PV structures, with a percentage of around 85%, while the remaining aluminum demand is used for wind turbine structures. This explains the similar trends for aluminum and other materials used for solar PV in the global food system.

Demand for critical materials as a percentage of their global primary production. The demand for critical materials was studied to assess the impact of the cellular agriculture transition accompanied by the use of green energy on the global primary sources of critical materials. Results demonstrated the need for additional input of several critical materials ranging between 0.03% to 35% of current world primary production levels (Supplementary Fig. 8). Among the critical materials required for the wind energy sector, the demand percentage of REEs is the highest, including dysprosium, neodymium, praseodymium, and terbium, with increases reaching up to 9–17% of their primary production in 2050 for a total replacement scenario (Supplementary Fig. 8). REEs mining is strongly affected by the growth of green technology propagation, as a 1% increase in green energy capacities can cause 0.18% depletion of REE reserves¹⁵. The boron demand for wind turbines represents a small percentage of its global primary production. This is mainly due to the limited amount of boron used in wind energy systems⁴⁴. The demand for structural materials in 2050, including aluminum, manganese, and zinc, increases and accounts for around 0.1%, 0.17%, and 1.9% of their total global primary production, respectively, given a total replacement scenario. The low demand percentages relative to the materials are due to the variety of purposes these structural materials can serve outside the energy industry. Around 90% of global manganese consumption is accounted for the production of multiple steel-grade structures⁴⁵. The use of manganese in the wind turbine industry is limited to the inclusion of steel to support the turbine structures, accounting for around 1.6% of steel weight⁴⁶. Despite the highest contribution of zinc to wind energy

in the food system, among other critical materials, most mined zinc material is used in the construction sector in the form of zinc coatings for galvanized steel (>90%)⁴⁷. Most of the produced aluminum is used for the building and construction sector, transportation, electronics, appliances, machinery, and equipment, accounting for more than 95% of total primary production⁴⁸.

The demand for key critical materials needed for solar PV in the food system is projected to increase by 2050, reaching up to 34% of the current global primary production of tellurium, given a total replacement scenario (Supplementary Fig. 8). The solar PV industry uses Tellurium heavily, comprising up to 40% of global production⁴⁹. Similarly, germanium demand accounts for 19% of total germanium primary production, as most of the produced material is used in the semiconductor industry, particularly in the manufacturing of solar cells⁵⁰. The demand for other key critical materials, i.e., gallium, indium, and silicon, accounts for lower percentages of their global production (1.6–21%). Despite the importance of silicon in the solar industry, where over 85% of current solar cells are based on silicon, >80% of silicon is used to produce silicone materials, superalloys, and cast iron⁵¹. The global primary production of gallium is often driven by the manufacturing of integrated circuits and laser diodes (>95%), while only <2% is used in the manufacturing of solar cells, mainly corresponding to CIGS technologies⁵². The global primary production of indium is mostly driven by the production of indium-containing alloys, compound semiconductor materials, and indium-tin oxides. The remainder is used for the manufacturing of CIGS cells for solar systems, accounting for less than 1% of global consumption⁵³.

When wind energy is used in cellular agriculture, the demand for chromium and nickel declines. The total elimination of livestock production, including dairy, will decrease the primary production demand of those minerals by 13% by 2050, considering the adoption of wind energy sources to the cellular agriculture transition activities. On the other hand, the demand for chromium and nickel in 2050 will increase, reaching up to 2% and 23% of their global primary productions, respectively, when solar energy sources are adopted in order to achieve a complete transition to cellular agriculture. These increases are driven by 14% higher material intensity of stainless steel in solar panels than in the dairy industry.

The primary production of phosphate rock—the elemental form of phosphorus—is increasingly driven by the growth of population and changes in lifestyle¹⁸, reaching up to 1.3 times the current primary production by 2050, given current livestock production practices (Supplementary Fig. 8).

Demand for critical materials versus their primary production capacity. The level of demand for critical materials as a result of the transition to cellular agriculture was analyzed with regard to the associated capacity of their production. The results indicate that despite the increase in critical material demand to achieve a full transition to cellular agriculture by 2050, 100% transition can take place without exceeding the existing primary production capacity levels for most materials (Fig. 6).

In the case of cellular agriculture transition powered by solely wind energy, the additional amount of the mined materials is not anticipated to exceed the primary production capacity for any of the associated elements, i.e., aluminum, boron, dysprosium, neodymium, nickel, praseodymium, terbium, and zinc. On the other hand, the demand for tellurium, mainly driven by the generation of energy by solar PV, will lead to a 34% increase in the current primary production that allows a maximal 60% transition to cellular agriculture by 2050. The maximum capacity

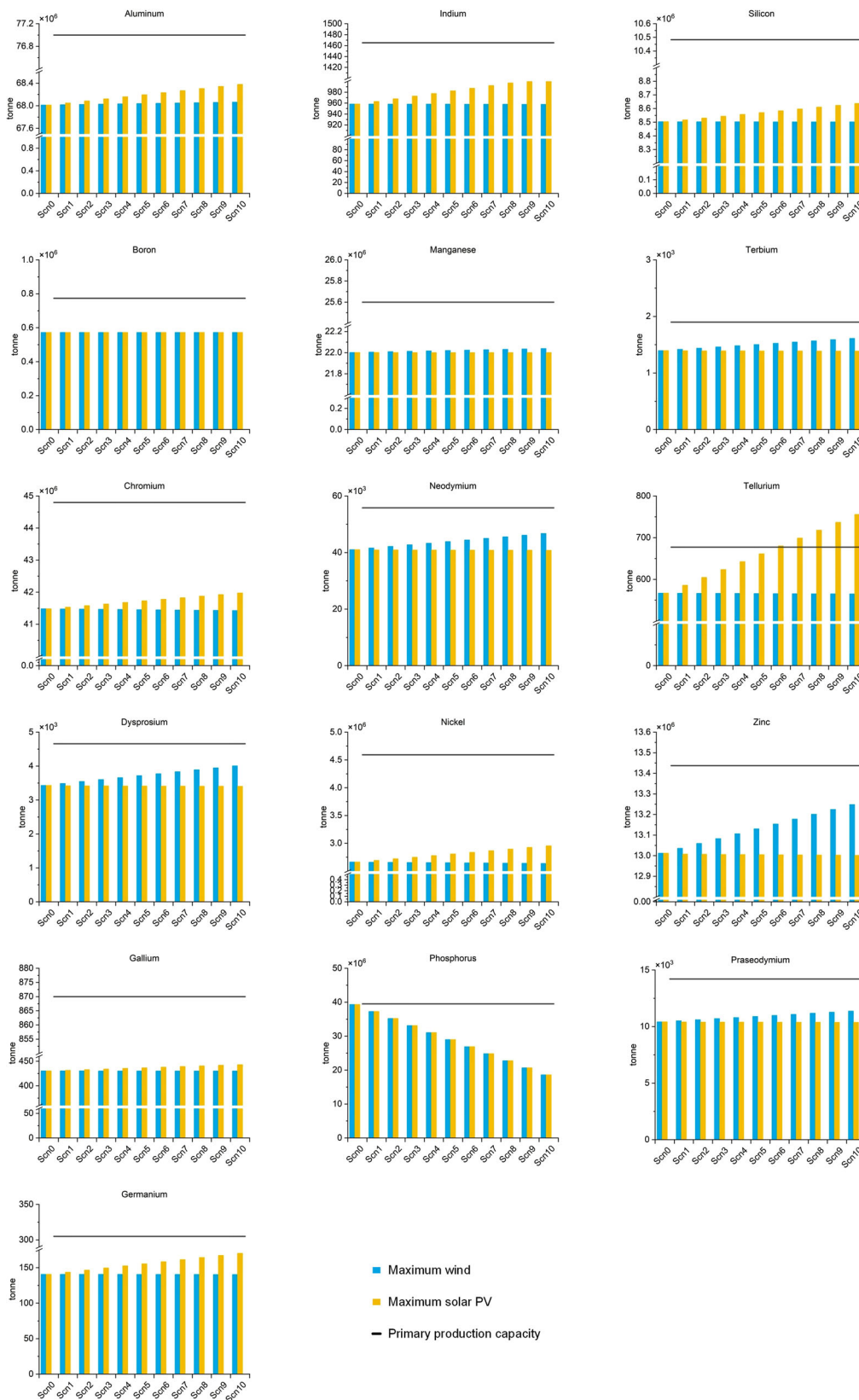


Fig. 6 Primary production of critical materials in 2050 to meet the global demand including the global food system requirements under different replacement scenarios (Scn0→Scn10). The blue bars correspond to the replacement solely powered by wind energy, the orange bars correspond to the replacement solely powered by solar PV, and the horizontal black line corresponds to the current primary production capacity level.

of Te primary production is around 673 tonnes. This finding highlights the need for PV technology improvement in use and recycling for critical materials recovery. With current livestock production practices, phosphorus primary production will reach its maximum capacity by 2050—39 million tonnes. It should be stressed that phosphorus is the only critical material for which a total transition to cellular agriculture can lead to a decrease of the demand below its primary production capacity, meaning a decrease of 53% by 2050.

The estimated primary production capacities of several critical materials will be higher than their world demand in 2050, including zinc (1%), chromium (6%), aluminum (13%), boron (35%), manganese (17%), indium (53%), silicon (21%), REEs (37%), nickel (55%), gallium (96%), and germanium (79%).

Sensitivity analysis. A sensitivity analysis was conducted to examine the spectrum of changes in the main results. Two parameters among the cellular agriculture production acted as the dependent variables: (1) electricity consumption with an input increase of 20%, and (2) glucose production with an input increase of 20%. Details on the sensitivity analysis modelling can be found in Supplementary Method 2. The inventory inputs can be found in Supplementary Data 9–11 for the cell-cultured RP, and Supplementary Data 13 for the MP. The results showed limited impact and no change to overall conclusions. The increase in glucose inputs increased GHG emissions, agriculture land use, and the consumption of primary phosphorus by 1.3%, 1.2%, and 2.6%, respectively. Increasing the electricity inputs had the highest impact on the consumption of the studied critical materials, with 19–20% increase in demand for wind turbine and solar PV-related materials. Nickel and chromium consumption increased by 11% following the increase in electricity inputs. With the condition of increasing the electricity consumption by 20%, the world demand for Te reaches the maximum capacity limits with a 50% transition to cellular agriculture by 2050. Details on the sensitivity analysis results can be found in Supplementary Data 14. To ensure the accuracy of the model, the comparison between the model and real-world data showed at least 95% compatibility, i.e., P primary production, fertilizers production, agriculture land use, and GHG emissions from food production. Details on the percentage accuracy calculations and annual results can be found in Supplementary Method 5.

Discussion

The findings proved the possibility of utilizing solely wind or solar PV technologies in the transition to cellular agriculture globally. However, the combination of these technologies to power the global transition to cellular agriculture could bring flexibility and optimize the consumption pattern of the required critical raw materials. In addition, combining both sources could overcome the potential limitations on the regional levels, i.e., national and regional capacity limits of wind and solar PV energy sources. The integrated approach will be promising for the sustainable development of cellular agriculture on a global scale.

In this work, the environmental data collected for livestock and crop production referred to the mean values reported in Poore and Nemecek³⁶. The results of Poore and Nemecek³⁶ demonstrated the high range of impacts on the production of livestock and crop commodities. Beef herd had generally the highest range of impacts with the 90th percentile being 5.25 times higher than the 10th percentile for GHG emissions, while the 90th percentile of land use was 8.8 times higher than the 10th percentile for the same product. This range of impacts contributes further to the uncertainty of the environmental benefits of the global food system in light of the global transition to cellular agriculture.

Carbon dioxide (CO₂) emissions generally persist in the atmosphere for millennia, forming an accumulating stock without a clear removal process. On the other hand, other climate pollutant emissions have comparatively shorter life spans, i.e., methane (CH₄), despite the immediate environmental damage they cause in the short term⁵⁴. When differentiating between the different gas types in the studied model, the overall CO₂ emissions followed an increasing trend following the replacement progress of livestock with cellular agriculture by the year 2050. On the contrary, CH₄ emissions experienced a decreasing trend following the gradual decline in livestock production activities by the year 2050 (Supplementary Discussion 3, Supplementary Fig. 5). Detailed calculations of the CH₄ and CO₂ emissions can be found in Supplementary Data 16–19. The 30-year period of the studied dynamic model (2020–2050) does not allow a conclusive statement on the long-term environmental costs or benefits of the livestock replacement model with cellular agriculture, as Lynch et al.⁵⁴ report a period of 50 years before emissions and removals of CH₄ are approximately balanced.

Our research focused on replacing livestock products as a source of protein, without considering the by-products of animal production (i.e., fat, leather, organs, pet food, medicine, lubricants, and chemicals). The elimination of the studied livestock main products (i.e., dairy, eggs, and meat from the studied livestock species) from the protein production model and replacing them with cellular agriculture products leads to the elimination of livestock by-products. The impacts of by-product replacement on the environment (i.e., GHG emissions, land use, energy consumption) and resource consumption (i.e., critical materials) were not analyzed.

The protein structure of the cellular agriculture products, i.e., MP and cell-cultured RP, is close to the respective animal-based protein sources⁵⁵. The studied products contain all nine essential amino acids required by the human body. The ingredient lists provided for the microbial proteins (MP) and cell-cultured recombinant proteins (RP) production show the existence of certain nutrients essential for the healthiness of the food products, i.e., sodium, potassium, phosphorus, magnesium, sulfur, calcium, manganese, iron, zinc, and copper²⁹. The comparison of the nutrient profile of the studied cellular agriculture products and livestock sector (nutrition data derived from the USDA⁵⁶) showed that livestock products had higher nutrient contents, e.g., beef contained at least five times higher iron quantities and at most 425 times higher zinc quantities than MP when comparison was done based on the protein content. Hence, the transition from livestock to the studied cellular agriculture products would require more changes in diets to ensure sufficient intake of all essential nutrients.

The final output of the studied cellular agriculture products is flour-like powder, which is different from the various livestock commodities, i.e., meat, dairy, and eggs. Therefore, the powder requires further processing and mixing with plant-based ingredients to make processed replacement products for livestock products. The additional impacts of the processing were not considered in this study. However, this is in line with the system boundaries of the livestock products, as only the processes up to the farmgate were included.

This work presented the environmental and resource consequences of replacing livestock with cellular agriculture at a global level. The findings do not serve the idea of recommending a specific diet to be followed based on the obtained results. This work did not examine the flexibility of switching to different food alternatives, i.e., cellular agricultural products. Previous research has discussed the inclusion of various food alternatives to replace livestock products, showing potential benefits regarding nutrition, environment, and accessibility^{57,58}. The results of this work can

be utilized in future research as a criterion to study the different replacement alternatives of livestock-based diets.

Despite the existence of discovered reserves, in large quantities for some materials, the development of mining activities often relies on other factors, i.e., technological advancement, market economy, and the associated costs, including energy and operating costs⁵⁹. In addition, some materials are refined as by-products of other mined materials, i.e., tellurium, which is refined due to copper mining and extraction. Despite the economic importance of tellurium in the sectors studied in this work, such as the solar PV industry, the future extraction of tellurium is often driven by the main purpose of obtaining copper and not based on the availability of tellurium reserves, where copper producers are less eager to invest in the recovery of additional tellurium⁶⁰. Currently, the scaled recycling of some critical materials in the green energy sector is far from developed⁶¹. For example, the recycling rate of neodymium magnets used in wind turbines is still less than 1%⁶². With this level of uncertainty surrounding the estimations of the future availability of critical materials used in the green energy sector, this work considered the mine capacity, which is the maximum possible output of annual mined materials based on current economic and technological conditions. However, future research should incorporate the development of critical material extraction in addition to the current limitations.

The prices associated with green energy technologies, i.e., solar PV and wind turbines, have followed a declining trend for the last decade, where the latest global prices per 1 MW in 2021 reached around 0.8 million USD and 0.25 million USD from wind turbines and solar PVs, respectively⁶³. However, the reversal of the cost reduction trend since the beginning of 2021 led to an increase in prices for wind turbines and solar PV modules⁶⁴. This was partially driven by the increase in prices of raw materials, including several critical elements, where the latest prices of REEs, nickel, and aluminum increased 2.5, 3.1, and 1.8 times, respectively, compared to 2017 prices⁶³. While the increase in prices in the green energy sector was driven by growth in demand, this might lead to the rebound effect of lower demands in the future. The studied model adopts the projections of increased green energy capacities by the year 2050¹⁰. However, the price fluctuations and the supply-demand dynamics may create uncertainties in capacity projections. Future research is encouraged to conduct a deeper analysis considering the prices of the various material inputs and the possibility of substitutes for the most expensive elements.

The desired reduction of land used for livestock farming offers new areas for natural vegetation and restoration of biodiversity. However, some land types used originally for grazing, i.e., marginal lands, hold neither agricultural nor industrial value⁶⁵. This work lacks the categorization of land types to draw a clear estimation of the environmental costs and benefits following grassland use reduction. A clear differentiation between the different agriculture lands used for livestock production is needed to have a clear overview of the environmental consequences of livestock replacement with cellular agriculture.

Most studies on the processes of cellular agriculture production are still on a laboratory scale. The future of scaled-up cellular agriculture production remains vague and holds many uncertainties regarding the wide changes in the inventory inputs and the market situation.

Methods

System dynamics modeling. We applied a global dynamics model of transition to cellular agriculture using a system dynamics (SD) modelling⁶⁶ combined with life-cycle assessment

(LCA). All inputs of the model, the model structure, and model validity can be found in Supplementary Tables 3, 4, and 2.

The integration of both methods enables examination of the current environmental situation by taking into account various feedbacks and loops⁶⁷. SimaPro PhD software was used to perform LCA analysis, and Vensim PLE software was used for the system dynamics modelling.

The food system is complex as causal relationships take place externally between socio-economic factors and streams of commodities, and internally between the flows of different commodities (i.e., crops and feed production, livestock production, fertilizer production)⁶⁸. These interactions result in the distinctive behavior of the food system. In addition, the different stages of food production contribute to changes in the energy supply systems and, consequently material systems⁶⁹. The use of a system dynamics model was motivated by the need to overcome some of the limitations of the model food systems, as model food systems lack the ability to understand the mechanisms behind the consequences or effects of changes in input parameters⁷⁰. Assessing complex systems involving material, energy, food, and environmental consequences requires the consideration of various mechanisms and factors, for example, delay mechanisms, including time lags in various processes and feedback loops; dynamic market factors, including supply and demand and price fluctuations; geographical-based production; and scenario analysis. System dynamics modelling allows us to understand the structure of the system and to analyze the behavior of variables influenced by several policies over time⁷¹. System dynamics modelling analyzes multi-systems given their established relationships⁷². The analysis covered a 30-year time horizon (2020–2050). The selection of this time interval is motivated by an intention to explore the changes that cellular agriculture could bring in line with the global roadmap of energy transformation by 2050. The aim of the global roadmap is to limit the rise of global average temperature to well below 2 °C above pre-industrial levels, mainly by carbon sequestration and decarbonization measures, including the deployment of low-carbon technologies based on renewable energy sources⁸.

Stocks and flows are the foundations of system dynamics modelling. Stock (i.e., stock of material or energy) corresponds to an entity that accumulates or drains over time, as shown in Eq. 1.

$$S(t) = t_0 t \int [I(t) - O(t)] dt + S(t_0) \quad (1)$$

where, $S(t)$ is the amount of material accumulated at time t ; $I(t)$ and $O(t)$ are calculated using Eq. 2. $I(t)$ is the amount of material input to $S(t)$ at time t ; $O(t)$ is the amount of material output from $S(t)$ at time t ; and $S(t_0)$ is the amount of material accumulated at the initial time t_0 .

$$\begin{aligned} I(t) &= f(S(t), V(t), P); \\ O(t) &= f(S(t), V(t), P) \end{aligned} \quad (2)$$

where $V(t)$ is an auxiliary variable (i.e., it is not directly affected by the system components) at time t , e.g., the supply flow of secondary fertilizers depends on the organic wastes from food consumption and livestock, and the available stock of organic wastes; P is a parameter of the system, e.g., recovery coefficient of wastes to secondary fertilizers.

The dynamics of the system will be driven by the annual global production of food until the year 2050, affected by socio-economic developments leading to the future increase of the demand for crops and livestock⁷³. The produced quantities of food commodities were derived from the database of the Food and Agriculture Organization of the United Nations (FAO)⁷⁴, while considering the annual growth of population from the United Nations (UN)–population division⁷⁵, and the projections

by 2050 of per capita consumption from the reports published by FAO for livestock meat, dairy, eggs, cereals, vegetables, and fruits^{76,77}. The global projections in the report applied the categorization of countries into “developing” and “developed” based on gross domestic product (GDP) levels.

System description of the food supply chain. In this study, the global food system was designed following the magnitude of nutrient flows, i.e., phosphorus. Phosphorus plays a fundamental role in the food production–consumption chain where agriculture primarily depends on the inputs of phosphate nutrients⁷⁸. The boundary of the studied system encompassed: (1) extraction, beneficiation, and processing of nutrients; (2) production of fertilizers and chemical feed; (3) production of crops as food and feed commodities (i.e., fruits, vegetables, rice, wheat, maize, barley, rye, sugarcane, and oat); (4) production of cellular agriculture (i.e., MP and cell-cultured RP) and livestock (i.e., beef, lamb, pork, poultry, milk, cheese, and eggs); (5) agriculture waste generation; and (6) downstream processes, i.e., waste disposal, landfilling, and recycling. The analysis of food products followed the cradle-to-gate approach (farmgate for crops and livestock products), excluding the packaging, retail, marketing, preparation, and distribution processes.

The first stage in food production refers to the input of nutrients, i.e., phosphorus. Phosphorus originates from the non-renewable natural resource—phosphate rock—that undergoes several stages of refining following mining activities, beneficiation, and processing. Processed nutrients are next used to produce fertilizers as well as food and feed additives, while the rest is used for non-agricultural purposes such as detergent and various industrial products¹⁸.

Fertilizers—mainly in the form of diammonium and monoammonium phosphates—are applied directly to the soil to enhance the yield and productivity of crops. The uptake of phosphorus nutrients per crop type was derived from Chen and Graedel⁷⁹. Historical statistics show that up to 40% of cereal production is driven by livestock demand and is directly utilized for livestock farming⁴⁰. The remaining crop production is destined for the human consumption although some yield is also used as feed for livestock farming⁷⁹.

Pork and poultry have been dominant in the meat production industry, where 37% and 35% of meat originates from pork and poultry species, respectively. Around 21% of meat comes from beef and cattle, while the rest comes from sheep, goat, horse, camel, and duck⁸⁰. In the dairy industry, cattle and buffalo contribute to >95% of global milk production, while the rest originates from goat, sheep, and camel⁸¹. Around 30% of the globally produced milk is used for cheese production based on protein content⁷⁴, by considering 3.5% and 25% of protein content in cow milk and cheese, respectively^{82,83}. The data on phosphorus contents in meat varieties, dairy, and egg products were obtained from the U.S. Department of Agriculture (USDA)⁵⁶. For poultry production, chicken meat was used as it accounts for more than 90% of total poultry meat globally⁸⁴.

After food production from livestock and crop origins, ~30% of products ready for consumption are wasted on an annual basis⁸⁵. Concerning livestock production, 10% goes to the consumption stage, while the rest ends up as waste, 90% of which is used as organic fertilizers for direct application on croplands in the form of animal manure⁷⁹. Beside the flows of manure, recycled nutrients from wastewater are also used as organic fertilizers^{86,87}.

Nutrient losses occur throughout the food supply chain. Mining, beneficiating, and processing of raw natural resources of phosphorus lead to 28% losses⁸⁸. During agricultural production, runoff of nutrients from the soil is the main reason for

phosphorus losses to marine ecosystems (around 28% of total nutrient input to the soil)⁷⁹. This runoff phenomenon is driven by the leaching of excess nutrients that are not absorbed by crop plants, leading to the accumulation of phosphorus in water⁸⁹. Contamination of water surfaces arises from animal waste, feeding operations, food consumption, crop harvesting, and wastewater treatment processes^{79,90}.

Cellular agriculture production. The production of cellular agriculture was based on the protein content of livestock products. The protein content for chicken broiler, beef, pork, lamb, egg, cow milk, and cheese was derived from the USDA⁵⁶.

In this study, phosphorus inputs were obtained from the production of phosphoric acid after beneficiating and processing primary material from extracted phosphate rock. Approximately 20% of phosphorus input to MP and cell-cultured RP was released to wastewater streams, following the calculations by Järviö et al.²⁹, with regard to the wastewater generation phase after the fermentation during the MP production process. The recovery processes for wastewater were included in the production system. By extension, the calculations of the environmental indicators (i.e., energy demand and GHG emissions) encompassed the recovery processes.

Mathematical model of food production. In the model, the world production of crop products is calculated as the production of crops per capita multiplied by the population⁹¹ ($Cp(t)$) as follows (Eq. 3):

$$Cp(t) = P(t) \times c(t) \quad (3)$$

where $P(t)$ is the world population at time t ; $c(t)$ is the annual crops production per capita at time t . Livestock production depends on livestock demand and the replacement coefficient with cellular agriculture products. In this step, livestock demand was calculated based on protein contents as cellular agriculture transition was based on protein replacement. The protein contents of the livestock products were derived from the USDA⁵⁶. Equation 4 corresponds to livestock protein demand ($D_i(t)$) at time t .

$$D_i(t) = P(t) \times d_i(t) \quad (4)$$

where $d_i(t)$ is demand of livestock product protein $i = 1, 2, 3, \dots, 7$ (beef, lamb, pig meat, poultry, milk, cheese, and eggs) per capita at time t . The production of cellular agriculture depended directly on the livestock protein demand ($D_i(t)$) and the replacement coefficient ($q_\alpha(t)$) at time t . For livestock meat proteins, MP ($mp(t)_i$) and cell-cultured RP ($rp(t)_i$) proteins are produced to totally replace livestock protein products (Eq. 5):

$$\begin{aligned} mp(t)_{i(1 \rightarrow 4)} &= \frac{1}{2} \times D_i(t) \times q_\alpha(t); \\ rp(t)_{i(1 \rightarrow 4)} &= \frac{1}{2} \times D_i(t) \times q_\alpha(t) \end{aligned} \quad (5)$$

cell-cultured RP is produced to replace only dairy and egg products (Eq. 6):

$$rp(t)_{i(5 \rightarrow 7)} = D_i(t) \times q_\alpha(t) \quad (6)$$

Description of energy consumption system. The World Food LCA database³⁷ and Agri-footprint 5.0³⁸ were utilized to calculate the energy requirements for the production of crops. (Details on the inventory data and energy values can be found in Supplementary Method 3, Supplementary Tables 1 and 4). The total energy demand covered the cradle-to-farmgate processes. Only crops meant for human consumption were included in this category, while the energy needed for feed crops was included in the livestock production sector. The energy required for the

livestock meat, milk, and eggs production was derived from Vries and Boer⁹², where 16 peer-reviewed works on the environmental impact of livestock production were analyzed by cradle to farmgate LCA. Studies encompassed OECD countries, as the use of livestock animals was driven by the demand for livestock food products. The average consumption of energy was determined and used in our model. The energy requirements for cheese to the farmgate was derived from Finnegan et al.⁹³. The study reviewed five assessments of the cumulative energy demand of cheese production in Netherlands, USA, Spain, and Portugal.

The energy requirements for cellular agriculture were derived from Järviö et al.^{29,30}—53 kWh per kg MP and 44 kWh per kg cell-cultured RP proteins. Further information on the total energy demand of cellular proteins can be found in Supplementary Fig. 2.

The energy requirements for nutrients recovery from wastewater were derived from Spångberg et al.⁹⁴. Energy consumption is associated with two subsequent methods, ‘thermo-chemical treatment’ and ‘wet chemical approach’⁹⁵. The ‘thermo-chemical treatment’ is meant to remove heavy metals from sludge phases via addition of chloride additives. This facilitates the extraction of phosphorus from those sludge phases via the ‘wet chemical approach’ by adding strong acids⁸⁶.

The general mathematical formulation of energy consumption ($E_b(t)$) in the food system is a follows (Eq. 7):

$$E_b(t) = p_b(t) \times e_b \quad (7)$$

where e_b is the energy demand per tonne product b ; and $p_b(t)$ is the production of product b at time t .

Greenhouse gas (GHG) emissions. The assessment of GHG emissions considered the carbon equivalent emissions from primary production of nutrients, fertilizers, crops, livestock meat, dairy, and eggs, recycling of nutrients, and production of cellular agriculture products.

The study by Poore and Nemecek³⁶ was taken as reference for the carbon footprint per tonne product of livestock and crops. The global mean data of the analyzed studies was used for the global assessment. The percentage accuracy of the obtained results can be found in Supplementary Method 5. The system boundary of the study was up to the retail stage. We excluded the emissions in post farmgate stages, which constituted around 17% of total GHG emissions from the food system. The GHG emissions associated with agriculture product ($G_1(t)$) at time t are calculated as follows (Eq. 8):

$$G_1(t) = \sum_{i=1}^I ghg_i \times p_i(t) \quad (8)$$

where ghg_i is the intensity of GHG emissions per tonne product i (Supplementary Table 4); and $p_i(t)$ is the production of product i at time t .

The GHG emissions associated with cellular agriculture ($G_2(t)$) at time t are calculated with Eq. 9 as follows:

$$G_2(t) = \sum_{b=1}^2 g_b \times \varphi_b(t) \quad (9)$$

where g_b is the intensity of GHG emissions per tonne of cellular agriculture proteins $b = 1, 2$ (MP and cell-cultured RP); and $\varphi_b(t)$ is the amount of the production of cellular agriculture protein b at time t .

For the recycling stage of nutrients, GHG emissions are estimated based on the energy consumed during recovery operation using three streams: wastewater, manure, and solid wastes. The global distribution of utilized energy sources was adopted to allocate the energy mix for the recycling operations.

The latest results showed the following distribution of global energy consumption according to the energy source: petroleum oil (31%), natural gas (24%), coal (27%), hydroelectrical (7%), nuclear (4%), and wind and solar PV (7%)³⁵.

The calculation of generated GHG emissions from nutrient recycling ($G_3(t)$) at time t is calculated using Eq. 10.

$$G_3(t) = \sum_{x=1}^X J_x(t) \times \varnothing_x \quad (10)$$

where $J_x(t)$ is the energy consumption in recycling process at time t from energy source x ; and \varnothing_x is the intensity of GHG emissions per one kilowatt hour energy consumed from source x . GHG emissions from different energy sources can be found in Supplementary Table 4.

Agricultural land use. In this study, agriculture land consisted of land for production of crops (arable land) and land for livestock grazing (pasture and grassland). Poore and Nemecek³⁶ was used as reference as they provided detailed results on the agriculture land demands per unit of food product (Supplementary Table 4). Land use for livestock production refers mainly to the cultivation of feed crops and grazing activities of animals. Hence, the land use for livestock meat also included the land requirements for feed crop cultivation on arable lands. The total land use for livestock production ($L_s(t)$) at time t is calculated by Eq. 11 as follows:

$$L_s(t) = \sum_{i=1}^I l_s_i \times p_i(t) \quad (11)$$

where l_s_i is the land use per tonne livestock product i ; and $p_i(t)$ is the production of product i at time t . The cropland area used for the production of crops for human consumption referred to the land requirements for the production of embodied nutrients in crops (i.e., P). Hence, cropland area used for food production ($L_a(t)$) at time t is calculated using Eq. 12 as follows:

$$L_a(t) = la \times a(t) \quad (12)$$

where la is the land area to produce one tonne of crop for food; and $a(t)$ is the amount of crops produced at time t . The total arable land used for the livestock production was derived from Poore and Nemecek³⁶, constituting a coefficient (c_b) of around 0.16 of total land requirements for livestock products. The coefficient reflects the share of arable land used for the production of all livestock species. It was assumed to be constant as the shares of meat production from different animal species are not subject to change until 2050⁷⁶. Equation 13 corresponds to land use for feed crops production ($L_b(t)$) and Eq. 14 corresponds to pasture land use at time t .

$$L_b(t) = c_b \times L_s(t) \quad (13)$$

$$L_p(t) = (1 - c_b) \times L_s(t) \quad (14)$$

The land use for cellular agriculture was derived from Järviö et al. publications on MP²⁹ and cell-cultured RP³⁰, given that the production is powered by green energy technologies (solar PV and wind). The arable land used in the cellular agriculture production ($L_c(t)$) is limited to the production of maize as a glucose source for cell-cultured RP, and is calculated as follows (Eq. 15):

$$L_c(t) = l_{RP} \times \varphi_2(t) \quad (15)$$

where l_{RP} is the land use requirements per tonne of cell-cultured RP protein and $\varphi_2(t)$ is the amount of cell-cultured RP proteins at time t .

Equation 16 gives the arable land use as follows:

$$L_{arable}(t) = L_c(t) + L_b(t) + L_a(t) \quad (16)$$

Demand for infrastructure—green energy and stainless steel.

The demand for green energy and stainless-steel structures depended on factors including average lifetime of structure and requirements per resource flow. The studied model encompasses several technologies across the food system (mining, production, and recovery technologies), cellular agriculture system (microbial protein and cell-cultured recombinant technologies), and energy supply system (wind and PV solar technologies). Researchers have estimated that the development of green energy supply technologies showed changes in material intensities until 2050, mainly driven by the need for higher efficiency in production processes¹⁰. The amounts of materials required for the construction of wind turbines (i.e., zinc, nickel, chromium, aluminum, and manganese) showed a decreasing trend, while the amount of materials required for the function of wind turbines and solar PV panels showed an increasing trend (i.e., tellurium, germanium, gallium, indium, rare earth elements, and boron)¹⁰. It should be noted that the ratios could be adopted in the model based on a new identified technology or energy sources.

Equation 17 corresponds to the total amounts ($S_z(t)$) of unit z (i.e., solar PV panel, wind turbine, and tonne stainless steel) required for the food system.

$$S_z(t) = t_0 t \int [I_z(t) - O_z(t)] dt + S(t_0) \quad (17)$$

where Eq. 18:

$$I_z(t) = \begin{cases} \text{if } N_z(t) > S_z(t-1); & N_z(t) - S_z(t-1) \\ \text{else;} & 0 \end{cases} \quad (18)$$

and Eq. 19:

$$O_z(t) = \frac{S_z(t-1)}{l_z} \quad (19)$$

where $N_z(t)$ is the amount of unit z needed at time t ; and l_z is the average lifetime of unit z . For green energy structures, $N_z(t)$ was calculated using Eq. 20:

$$N_z(t) = n_z \times \varepsilon(t) \quad (20)$$

where n_z is the amount of unit z required per 1 kWh electricity (wind turbines, solar PV panels); and $\varepsilon(t)$ is the electricity generated from wind or solar energy sources for the food system at time t . For stainless-steel structures, $N_z(t)$ was calculated as follows (Eq. 21):

$$N_z(t) = \sum_{\vartheta=1}^3 n_{z,\vartheta} \times k_{\vartheta}(t) \quad (21)$$

where n_z is the amount of unit z (tonne stainless-steel) per tonne material flow at sector $\vartheta = 1, 2, 3$ (dairy products, cellular agriculture products, and nutrients for wastewater treatment); and $k_{\vartheta}(t)$ is the mass flow of material in sector ϑ at time t . Data on equipment requirements can be found in Supplementary Table 4.

Demand for critical materials in the food system. The material intensities for green energy technologies were derived from the European Commission publication on the materials demand for wind and solar PV technologies¹⁰. The equation below is used to calculate the critical material demand ($CM_{y,z}(t)$) at time t (Eq. 22):

$$CM_{y,z}(t) = cm_{y,z}(t) \times N_z(t) \quad (22)$$

where $cm_{y,z}(t)$ is the critical material content at time t per one unit $z = 1, 2$ (solar PV panel and wind turbine) (material intensity in solar panels and turbines can be found in Supplementary Table 4); For stainless-steel, 304 and 316 stainless-steel grades had no marked difference in using the critical material composition (1% difference for chromium and nickel). Hence, the average of material composition in each grade was taken for the model.

Country-level cellular agriculture production. The calculation of the cellular agriculture protein to replace livestock production at a country-level was based on the associated availability of wind and solar PV capacities, as the direct cellular production was aimed to be fueled by green energy technologies only.

First, the country-level green energy capacities in 2050 are derived from Ram et al.⁹⁶. Second, the country contribution to the world livestock protein production is calculated based on the latest country-level and world livestock production from FAO database⁷⁴. Third, the country-level livestock protein production by 2050 was calculated by multiplying the country contribution to the projected global production in 2050. Country-level data on livestock production and green energy capacities can be found in Supplementary Data 1 and 3, respectively. Fourth, the direct electricity needed for the country replacement with MP and cell-cultured RP (r_i) in 2050 was calculated using Eq. 23 as follows:

$$r_i = \sum_{b=1}^2 \rho_{b,i} \times e_b \quad (23)$$

where $\rho_{b,i}$ is the estimated amount of cellular agriculture proteins, in tonnes, used to totally replace livestock protein products in country i ; e_b is the direct electricity needed to produce one-tonne cellular agriculture product $b = 1, 2$ (MP and cell-cultured RP) in protein content, respectively. Considering the limited national capacities of wind and solar PV, the electricity consumption that a country i would be able to handle to replace livestock proteins with cellular agriculture (y_i) is calculated as follows (Eq. 24):

$$y_i = y_{w,i} + y_{s,i} \quad (24)$$

where $y_{w,i}$ is the electricity originating from wind energy sources and $y_{s,i}$ is the electricity originating from solar PV energy ones, which are calculated with Eqs. 25 and 26 as follows:

$$y_{w,i} = \text{if} \begin{cases} Q_{w,i} \geq r_i; & r_i \\ \text{else;} & Q_{w,i} \end{cases}, \quad (25)$$

$$y_{s,i} = \text{if} \begin{cases} Q_{s,i} < r_i - y_{w,i}; & Q_{s,i} \\ \text{else;} & r_i - y_{w,i} \end{cases}$$

when wind power technology is given the priority, and

$$y_{s,i} = \text{if} \begin{cases} Q_{s,i} \geq r_i; & r_i \\ \text{else;} & Q_{s,i} \end{cases}, \quad (26)$$

$$y_{w,i} = \text{if} \begin{cases} Q_{s,i} < r_i - y_{s,i}; & Q_{w,i} \\ \text{else;} & r_i - y_{s,i} \end{cases}$$

when solar PV power technology is given the priority. $Q_{w,i}$ and $Q_{s,i}$ denote the regional wind and solar PV energy capacities in country i , respectively. The total livestock protein products to be possibly replaced by country i with cellular agriculture (φ_i) in

Table 1 Primary production capacity of studied critical materials.

material	primary production capacity (tonnes)	year
Al	77000000	2021
B	773704	2021
Cr	44800000	2019
Ga	870	2021
Ge	305	2012
In	1465	2018
Mn	25600000	2020
Ni	4600000	2021
P	40000000	2025
REE	35300000	2011
Si	10500000	2018
Te	677	2021
Zn	13350000	2010

2050 was calculated as follows (Eq. 27):

$$\varphi_i = \frac{y_i}{r_i} \times \sum_{b=1}^2 \rho_{b,i} \quad (27)$$

Primary production capacities of critical materials. The primary production capacity of several materials was derived from the latest publications of USGS, including aluminum⁹⁷, chromium⁹⁸, indium⁵³, rare earth elements⁹⁹, gallium¹⁰⁰, nickel¹⁰¹, and tellurium⁴⁹. The Statista database was used for the primary production capacity of phosphorus¹⁰². While for other materials, data was collected from regional reports for major world primary producers, i.e., germanium¹⁰³, boron¹⁰⁴, manganese^{105,106}, zinc^{107–112}, and silicon^{51,113}. Detailed information on the aggregation of data presented (Table 1) can be found in Supplementary Method 4.

It is important to note that technological advancements and resource discoveries can also increase production capacities in certain cases. Additionally, the likelihood of capacity decrease varies for different materials and industries, as each has its own unique dynamics and influences.

Data availability

The authors declare that the data supporting the findings of this study are available within the article and its Supplementary Information files. Primary data for the mining of critical materials and their intensities in green energy technologies was obtained from the USGS¹² and Carrara et al.¹⁰. Primary data on the environmental impacts of livestock, crops, and cellular agriculture products was obtained from Poore and Nemecek³⁶, World Food LCA³⁷, Agri-footprint³⁸, Vries and Boer⁹², and Järviö et al.^{29,30}.

Code availability

Code for the system dynamics model can be found in Supplementary Information.

Received: 21 June 2023; Accepted: 17 January 2024;

Published online: 31 January 2024

References

- Xu, X. et al. Global greenhouse gas emissions from animal-based foods are twice those of plant-based foods. *Nat. Food* **2**, 724–732 (2021).
- Humpenöder, F. et al. Projected environmental benefits of replacing beef with microbial protein. *Nature* **605**, 90–96 (2022).
- Post, M. J. et al. Scientific, sustainability and regulatory challenges of cultured meat. *Nat. Food* **1**, 403–415 (2020).
- Tuomisto, H. L. & Teixeira De Mattos, M. J. Environmental impacts of cultured meat production. *Environ. Sci. Technol.* **45**, 6117–6123 (2011).
- Eibl, R. et al. Cellular agriculture: opportunities and challenges. *Annu. Rev. Food Sci. Technol.* **12**, 51–73 (2021).
- Sillman, J. et al. Bacterial protein for food and feed generated via renewable energy and direct air capture of CO₂: can it reduce land and water use? *Glob. Food Sec.* **22**, 25–32 (2019).
- Mattick, C. S. Cellular agriculture: the coming revolution in food production. *Bull. At. Sci.* **74**, 32–35 (2018).
- IRENA. IRENA (2019). Global energy transformation: a roadmap to 2050. Global energy transformation. A roadmap to 2050 (2019).
- Pommeret, A., Ricci, F. & Schubert, K. Critical raw materials for the energy transition. *Eur. Econ. Rev.* **141**, 103991 (2022).
- Carrara, S., Alves Dias, P., Plazzotta, B. & Pavel, C. Raw materials demand for wind and solar PV technologies in the transition towards a decarbonised energy system. EUR 30095 EN, Publications Office of the European Union, Luxembourg (2020).
- El Wali, M., Golroudbary, S. R. & Kraslawski, A. Circular economy for phosphorus supply chain and its impact on social sustainable development goals. *Sci. Total Environ.* **777**, 146060 (2021).
- USGS. U.S. Geological survey release 2022 list of critical minerals. <https://www.usgs.gov/news/national-news-release/us-geological-survey-releases-2022-list-critical-minerals> (2022).
- EU Commission. CRM list 2020. <https://rmis.jrc.ec.europa.eu/?page=crm-list-2020-e294f6> (2020).
- Rankin, W. J. Minerals, metals, and sustainability: meeting future material needs. *Choice Rev. Online* **49**, (2012).
- Golroudbary, S. R., Makarava, I., Kraslawski, A. & Repo, E. Global environmental cost of using rare earth elements in green energy technologies. *Sci. Total Environ.* **832**, 155022 (2022).
- Tuomisto, H. L. Challenges of assessing the environmental sustainability of cellular agriculture. *Nat. Food* **3**, 801–803 (2022).
- Hashempour-Baltork, F., Khosravi-Darani, K., Hosseini, H., Farshi, P. & Reihani, S. F. S. Mycoproteins as safe meat substitutes. *J. Clean. Product.* **253**, 119958 (2020).
- Golroudbary, S. R., El Wali, M. & Kraslawski, A. Environmental sustainability of phosphorus recycling from wastewater, manure and solid wastes. *Sci. Total Environ.* **672**, 515–524 (2019).
- Balaram, V. Rare earth elements: A review of applications, occurrence, exploration, analysis, recycling, and environmental impact. *Geosci. Front.* **10**, 1285–1303 (2019).
- Grandell, L. & Höök, M. Assessing rare metal availability challenges for solar energy technologies. *Sustainability* **7**, 11818–11837 (2015).
- Bellani, C. F. et al. Scale-up technologies for the manufacture of adherent cells. *Front. Nutr.* **7**, 178 (2020).
- Issf. Stainless steel in the dairy industry a sustainable solution for human diet. **6**, 6–71 (2010).
- Euro Inox. Performance of stainless steels in waste water installations. materials and applications. *Series 13* www.turkpasder.com (2010).
- Turkbay, T., Bongono, J., Alix, T., Laratte, B. & Elevli, B. Prior knowledge of the data on the production capacity of boron facilities in Turkey. *Clean. Eng. Technol.* **10**, 100539 (2022).
- Rischer, H., Szilvay, G. R. & Oksman-Caldentey, K. M. Cellular agriculture — industrial biotechnology for food and materials. *Curr. Opin. Biotechnol.* **61**, 128–134 (2020).
- Hashempour-Baltork, F., Hosseini, S. M., Assarehzadegan, M. A., Khosravi-Darani, K. & Hosseini, H. Safety assays and nutritional values of mycoprotein produced by *Fusarium venenatum* IR372C from date waste as substrate. *J. Sci. Food Agric.* **100**, 4433–4441 (2020).
- Rubio, N. R., Xiang, N. & Kaplan, D. L. Plant-based and cell-based approaches to meat production. *Nat. Commun.* **11**, <https://doi.org/10.1038/s41467-020-20061-y> (2020).
- Ercili-Cura, D. & Barth, D. Cellular Agriculture. ACS In Focus, ACS Publications (2020).
- Järviö, N., Maljanen, N. L., Kobayashi, Y., Ryyänen, T. & Tuomisto, H. L. An attributional life cycle assessment of microbial protein production: a case study on using hydrogen-oxidizing bacteria. *Sci. Total Environ.* **776**, 145764 (2021).
- Järviö, N. et al. Ovalbumin production using *Trichoderma reesei* culture and low-carbon energy could mitigate the environmental impacts of chicken-egg-derived ovalbumin. *Nat. Food* **2**, 1005–1013 (2021).
- Matassa, S., Boon, N., Pikaar, I. & Verstraete, W. Microbial protein: future sustainable food supply route with low environmental footprint. *Microb. Biotechnol.* **9**, 568–575 (2016).
- Behm, K. et al. Comparison of carbon footprint and water scarcity footprint of milk protein produced by cellular agriculture and the dairy industry. *Int. J. Life Cycle Assess.* **27**, 1017–1034 (2022).
- Goldsmith, R. E. & Foxall, G. R. The Measurement of Innovativeness. In: The International Handbook on Innovation <https://doi.org/10.1016/B978-008044198-6/50022-X> (2003).

34. Kapur, A. & Graedel, T. E. Industrial ecology. *Encyclopedia of energy* 373–382 <https://doi.org/10.1016/B0-12-176480-X/00533-7> (2004).
35. British Petroleum. BP Statistical Review of World Energy, 2022. British Petroleum <https://www.bp.com/content/dam/bp/business-sites/en/global/corporate/pdfs/energy-economics/statistical-review/bp-stats-review-2022-full-report.pdf> (2022).
36. Poore, J. & Nemecek, T. Reducing food's environmental impacts through producers and consumers. *Science* **360**, 987–992 (2018).
37. Nemecek, T. et al. Methodological guidelines for the life cycle inventory of agricultural products, Version 3.0. World Food LCA Database at: (2015).
38. Van Paassen, M., Braconi, N., Kuling, L., Durlinger, B. & Gaul, P. Agri-footprint 5.0. (2019).
39. Dei, H. K. Assessment of maize (*Zea mays*) as feed resource for poultry. *In: Poultry Science* <https://doi.org/10.5772/65363> (2017).
40. Ritchie, H. If the world adopted a plant-based diet we would reduce global agricultural land use from 4 to 1 billion hectares. *Our World in Data* <https://ourworldindata.org/land-use-diets> (2021).
41. Dathu, K. P. M. Y. V. & Hariharan, R. Design of wind turbine blade material for higher efficiency. *Mater. Today: Proc.* **33**, 565–569 (2020).
42. Hernandez-Estrada, E. et al. Considerations for the structural analysis and design of wind turbine towers: a review. *Renew. Sust. Energ. Rev.* **137**, 110447 (2021).
43. International Energy Agency. Iron and steel technology roadmap: towards more sustainable steelmaking. Treatise on process metallurgy <https://www.iea.org/reports/iron-and-steel-technology-roadmap> (2020).
44. Brioche, A. S. 2018 Minerals Yearbook. Boron. <https://d9-wret.s3.us-west-2.amazonaws.com/assets/palladium/production/atoms/files/myb1-2018-boron-2.pdf> (2018).
45. Cannon, W. F. Manganese - it turns iron into steel (and does so much more). <https://pubs.usgs.gov/fs/2014/3087/pdf/fs2014-3087.pdf> (2014).
46. Igwemezie, V., Mehmanparast, A. & Kolios, A. Materials selection for XL wind turbine support structures: a corrosion-fatigue perspective. *Mar. Struct.* **61**, 381–397 (2018).
47. Tolcin, A. 2018 Minerals Yearbook - Zinc. <https://pubs.usgs.gov/myb/vol1/2018/myb1-2018-zinc.pdf> (2018).
48. Bray, L. 2018 Minerals Yearbook - Aluminum. <https://d9-wret.s3.us-west-2.amazonaws.com/assets/palladium/production/atoms/files/myb1-2018-alumi.pdf> (2018).
49. Anderson, S. *Tellurium*. <https://pubs.usgs.gov/periodicals/mcs2022/mcs2022-tellurium.pdf> (2022).
50. Thomas, C. 2018 Minerals Yearbook - Germanium. <https://d9-wret.s3.us-west-2.amazonaws.com/assets/palladium/production/atoms/files/myb1-2018-germa.pdf> (2018).
51. Schnebele, E. 2018 Minerals Yearbook - Silicon. <https://d9-wret.s3.us-west-2.amazonaws.com/assets/palladium/production/atoms/files/myb1-2018-simet.pdf> (2018).
52. Jaskula, B. 2018 Minerals Yearbook - Gallium. <https://pubs.usgs.gov/myb/vol1/2018/myb1-2018-gallium.pdf> (2018).
53. Anderson, S. 2018 Minerals Yearbook - Indium. <https://pubs.usgs.gov/myb/vol1/2018/myb1-2018-indium.pdf> (2018).
54. Lynch, J., Cain, M., Pierrehumbert, R. & Allen, M. Demonstrating GWP: a means of reporting warming-equivalent emissions that captures the contrasting impacts of short- and long-lived climate pollutants. *Environ. Res. Lett.* **15**, 044023 (2020).
55. Foods, S. Introducing Solein®. <https://solarfoods.com/solein/> (2023).
56. USDA. U.S. department of agriculture. <https://www.usda.gov/>.
57. Mazac, R. et al. Incorporation of novel foods in European diets can reduce global warming potential, water use and land use by over 80%. *Nat. Food* **3**, 286–293 (2022).
58. Mazac, R., Järviö, N. & Tuomisto, H. L. Environmental and nutritional life cycle assessment of novel foods in meals as transformative food for the future. *Sci. Total Environ.* **876**, 162796 (2023).
59. Michaux, S. P. The mining of minerals and the limits to growth. https://tupa.gtk.fi/raportti/arkisto/16_2021.pdf (2021).
60. Lusty, P. A. J. & Gunn, A. G. Challenges to global mineral resource security and options for future supply. *Geol. Soc. Spec. Publ.* **393**, 265–276 (2014).
61. EU Commission. Rare metals have huge potential for recycling in Europe. EU Commission <https://ec.europa.eu/research-and-innovation/en/projects/success-stories/all/rare-metals-have-huge-potential-recycling-europe> (2020).
62. Xia, D. et al. Sustainable route for Nd recycling from waste electronic components featured with unique element-specific sorting enabling simplified hydrometallurgy. *Chem. Eng. J.* **441**, 135886 (2022).
63. IEA. Critical Minerals Market Review 2023. <https://iea.blob.core.windows.net/assets/afc35261-41b2-47d4-86d6-d5d77fc259be/CriticalMineralsMarketReview2023.pdf> (2023).
64. IEA. Renewables 2021. Analysis and forecast to 2026. <https://iea.blob.core.windows.net/assets/5ae32253-7409-4f9a-a91d-1493fbf977a/Renewables2021-Analysisandforecastto2026.pdf> (2021).
65. Ramakrishna, W., Rathore, P., Kumari, R. & Yadav, R. Brown gold of marginal soil: plant growth promoting bacteria to overcome plant abiotic stress for agriculture, biofuels and carbon sequestration. *Sci. Total Environ.* **711** <https://doi.org/10.1016/j.scitotenv.2019.135062> (2020).
66. Forrester, J. W. Industrial dynamics. *J. Oper. Res. Soc.* **48**, 1037–1041 (1997).
67. Pinto, J. T. M., Sverdrup, H. U. & Diemer, A. Integrating life cycle analysis into system dynamics: the case of steel in Europe. *Environ. Syst. Res.* **8**, 1–21 (2019).
68. Purwanto, A., Sušnik, J., Suryadi, F. X. & de Fraiture, C. Using group model building to develop a causal loop mapping of the water-energy-food security nexus in Karawang Regency, Indonesia. *J. Clean. Prod.* **240**, 118170 (2019).
69. Ladha-Sabur, A., Bakalis, S., Fryer, P. J. & Lopez-Quiroga, E. Mapping energy consumption in food manufacturing. *Trends Food Sci. Technol.* **86**, 270–280 (2019).
70. Harper, W. J., Hewitt, S. A. & Huffman, L. M. Model food systems and protein functionality. *In: Milk proteins: from expression to food* <https://doi.org/10.1016/B978-0-12-815251-5.00015-3> (2019).
71. Groloudbary, S. R. & Zahraee, S. M. System dynamics model for optimizing the recycling and collection of waste material in a closed-loop supply chain. *Simul. Modell. Pract. Theory* **53**, 88–102 (2015).
72. Jia, B. et al. System dynamics model for the coevolution of coupled water supply–power generation–environment systems: upper Yangtze river Basin, China. *J. Hydrol.* **593**, 125892 (2021).
73. Fukase, E. & Martin, W. Economic growth, convergence, and world food demand and supply. *World Dev.* **132**, 104954 (2020).
74. FAOSTAT. Statistics on crops and livestock products. FAOSTAT <https://www.fao.org/faostat/en/#data/QCL> (2022).
75. UN DESA. World population prospects: The 2017 revision, key findings and advance tables. *United Nations* (2017).
76. Alexandratos, N. & Bruinsma, J. World agriculture towards 2030/2050. land use policy vol. 20 <https://ageconsearch.umn.edu/record/288998/> (2012).
77. FAO. The future of food and agriculture—Alternative pathways to 2050. Food and agriculture organization of the United Nations, Rome, Italy. Food and Agriculture Organization (2018).
78. Dai, Z. et al. Long-term nutrient inputs shift soil microbial functional profiles of phosphorus cycling in diverse agroecosystems. *ISME J.* **14**, 757–770 (2019).
79. Chen, M. & Graedel, T. E. A half-century of global phosphorus flows, stocks, production, consumption, recycling, and environmental impacts. *Glob. Environ. Change* **36**, 139–152 (2016).
80. Ritchie, H., Rosado, P. & Roser, M. Meat and dairy production. *Our World in Data* <https://ourworldindata.org/meat-production> (2017).
81. FAO. Gateway to dairy production and products. FAO <https://www.fao.org/dairy-production-products/production/dairy-animals/en/> (2022).
82. USDA. Milk, fluid, 1% fat, without added vitamin A and vitamin D. U.S. department of agriculture <https://fdc.nal.usda.gov/fdc-app.html#/food-details/173441/nutrients> (2019).
83. USDA. Cheese, cheddar (Includes foods for USDA's Food Distribution Program). U.S. department of agriculture <https://fdc.nal.usda.gov/fdc-app.html#/food-details/173414/nutrients> (2019).
84. FAO. Gateway to poultry production and products. FAO <https://www.fao.org/poultry-production-products/production/poultry-species/en/> (2023).
85. Rezaei, M. & Liu, B. Feature Articles. Food loss and waste in the food supply chain. *Nutfruit* **71**, 26–27 (2017).
86. Ye, Y. et al. Insight into chemical phosphate recovery from municipal wastewater. *Sci. Total Environ.* **576**, 159–171 (2017).
87. Pearce, B. B. J. & Chertow, M. Scenarios for achieving absolute reductions in phosphorus consumption in Singapore. *J. Clean. Prod.* **140**, 1587–1601 (2017).
88. Scholz, R. W., Hellums, D. T. & Roy, A. A. Global sustainable phosphorus management: a transdisciplinary venture. *Curr. Sci.* **108**, 1237–1246 (2015).
89. Ortiz-Reyes, E. & Anex, R. P. A life cycle impact assessment method for freshwater eutrophication due to the transport of phosphorus from agricultural production. *J. Clean. Prod.* **177**, 474–482 (2018).
90. Morillas-España, A., Lafarga, T., Sánchez-Zurano, A., Acien-Fernández, F. G. & González-López, C. Microalgae based wastewater treatment coupled to the production of high value agricultural products: current needs and challenges. *Chemosphere* <https://doi.org/10.1016/j.chemosphere.2021.132968> (2022).
91. Cordell, D., Drangert, J.-O. & White, S. The story of phosphorus: global food security and food for thought. *Glob. Environ. Change* **19**, 292–305 (2009).
92. de Vries, M. & de Boer, I. J. M. Comparing environmental impacts for livestock products: a review of life cycle assessments. *Livestock Sci.* <https://doi.org/10.1016/j.livsci.2009.11.007> (2010).
93. Finnegan, W., Yan, M., Holden, N. M. & Goggins, J. A review of environmental life cycle assessment studies examining cheese production. *Int. J. Life Cycle Assess.* <https://doi.org/10.1007/s11367-017-1407-7> (2018).
94. Spångberg, J., Tidåker, P. & Jönsson, H. Environmental impact of recycling nutrients in human excreta to agriculture compared with enhanced wastewater treatment. *Sci. Total Environ.* **493**, 209–219 (2014).

95. Appels, L., Degreve, J., Van der Bruggen, B., Van Impe, J. & Dewil, R. Influence of low temperature thermal pre-treatment on sludge solubilisation, heavy metal release and anaerobic digestion. *Bioresour. Technol.* **101**, 5743–5748 (2010).
96. Ram, M. et al. Global energy system based on 100% Renewable energy: power, heat, transport and desalination sectors. <https://resources.solarbusinesshub.com/images/reports/219.pdf> (2019).
97. Bray, L. Mineral Commodity Summaries 2022 - Aluminum. <https://www.trade.gov/aluminum> (2022).
98. Schulte, R. Mineral commodity summary - Chromium. <https://pubs.usgs.gov/periodicals/mcs2023/mcs2023-chromium.pdf> (2023).
99. Tse, P.-K. China's Rare-Earth Industry. <https://pubs.usgs.gov/of/2011/1042/of2011-1042.pdf> (2011).
100. Jaskula, B. Mineral commodity summaries 2023 - Gallium. <https://pubs.usgs.gov/periodicals/mcs2023/mcs2023-gallium.pdf> (2023).
101. McRae, M. Mineral commodity summaries - Nickel. <https://pubs.usgs.gov/periodicals/mcs2023/mcs2023.pdf> (2023).
102. Garside, M. Production capacity of phosphate rock worldwide from 2016 to 2020, with a forecast until 2025. *Statista* <https://www.statista.com/statistics/1288972/global-phosphate-rock-production-capacity/> (2022).
103. Melcher, F. & Buchholz, P. Current and future Germanium availability from primary sources. https://www.deutsche-rohstoffagentur.de/DERA/DE/Downloads/vortrag_germanium.pdf?__blob=publicationFile&v=2 (2012).
104. Borates. Country Profile - Boron Turkey. Borates today <https://borates.today/country-profile-boron-turkey/> (2021).
105. González, A. et al. Manganese matters. a metal of consequence for women and communities in South Africa affected by mining and the global energy transition. https://actionaid.nl/wp-content/uploads/2021/06/ActionAid_MangaanRaport_Lowres-FINAL.pdf (2021).
106. Mining data solutions. Manganese mining. Mining data solutions <https://miningdataonline.com/property/337/GEMCO-Mine.aspx#Mining> (2021).
107. Antaike. *Chinese Zinc Quarterly*. <https://www.antaike.com/uploadfiles/20150107/2015010715030470913.pdf> (2010).
108. Zinc, H. *Integrated Annual Report 2021-22*. [https://www.hzllindia.com/E-Annual-Report/2021-22/pdf/Annual Report 2021-22.pdf](https://www.hzllindia.com/E-Annual-Report/2021-22/pdf/Annual%20Report%2021-22.pdf) (2023).
109. Knapp, J. *Operation and Site Performance 2006*. https://www.teck.com/media/2006_Teck_Sustainability_Report_Red_Dog.PDF (2006).
110. NS Energy. Cerro Lindo Mine. *NS Energy* <https://www.nsenerybusiness.com/projects/cerro-lindo-mine/> (2021).
111. Dromundo, O. et al. Chapter 19: The Peñasquito Gold-(Silver-Lead-Zinc) Deposit, Zacatecas, Mexico. in *Geology of the World's Major Gold Deposits and Provinces* <https://doi.org/10.5382/sp.23.19> (2021).
112. MRM. *McArthur River Mining*. https://www.miningnewsfeed.com/reports/MRM_Fact_Sheet_03312017.pdf (2017).
113. Schnebele, E. *Mineral commodity summaries - Silicon*. (2023).

Acknowledgements

This work was supported by the Research Funds at the University of Helsinki and the 'Cultured Meat in the Post-animal Bioeconomy' project (no. 201802185) funded by the

KONE Foundation. We would like to thank Dr. Natasha Järviö for the valuable discussions on the production processes of microbial proteins and cell-cultured recombinant proteins.

Author contributions

M.E.W., S.R.G., A.K., and H.L.T. designed the work. M.E.W. and S.R.G. collected the data. M.E.W. created and validated the model. M.E.W. and S.R.G. carried out the data visualization and wrote the original draft of the manuscript. A.K. and H.L.T. reviewed and edited the manuscript. H.L.T. acquired the funding and supervised the work.

Competing interests

The authors declare no competing interests.

Additional information

Supplementary information The online version contains supplementary material available at <https://doi.org/10.1038/s43247-024-01227-8>.

Correspondence and requests for materials should be addressed to Mohammad El Wali or Saeed Rahimpour Golroudbary.

Peer review information *Communications Earth & Environment* thanks the anonymous reviewers for their contribution to the peer review of this work. Primary Handling Editors: Martina Grecequet. A peer review file is available.

Reprints and permission information is available at <http://www.nature.com/reprints>

Publisher's note Springer Nature remains neutral with regard to jurisdictional claims in published maps and institutional affiliations.



Open Access This article is licensed under a Creative Commons Attribution 4.0 International License, which permits use, sharing, adaptation, distribution and reproduction in any medium or format, as long as you give appropriate credit to the original author(s) and the source, provide a link to the Creative Commons licence, and indicate if changes were made. The images or other third party material in this article are included in the article's Creative Commons licence, unless indicated otherwise in a credit line to the material. If material is not included in the article's Creative Commons licence and your intended use is not permitted by statutory regulation or exceeds the permitted use, you will need to obtain permission directly from the copyright holder. To view a copy of this licence, visit <http://creativecommons.org/licenses/by/4.0/>.

© The Author(s) 2024